Indonesian Geotechnical Journal, December 2022, Vol 1 (3). Page 37 - 55
DOI: https://doi.org/10.56144/igj.v1i3.28
E-ISSN:2829-7520
https://indonesian-geotechnical-journal.org/index.php/IGJ/issue/archive

Liquefaction Potential Assessment for the City of Mamuju Sulawesi by using N-SPT based methods

Ardy Arsyad[1,4*], Andi Asti Nur Amaliyah[3], Sopian Paerong[3], Abdul Rahman Djamaluddin[2]
[1]Department of Civil Engineering, Faculty of Engineering, Hasanuddin University, Makassar, Indonesia, 90234; ardy.arsyad@unhas.ac.id
[2]Dept. of Civil Engineering, Faculty of Engineering, Hasanuddin University, Makassar, Indonesia, 90234
[3]Dept. of Civil Engineering, Faculty of Engineering, Hasanuddin University, Makassar, Indonesia, 90234
[4]Centre for Sulawesi Earthquake Studies, Makassar, Indonesia, 90172

SUBMITTED 30 November 2022 **REVISED** 28 December 2022 **ACCEPTED** 29 December 2022

ABSTRACT. Mamuju is the capital city of West Sulawesi Province which has experienced large earthquakes including the Majene Earthquake Mw. 6.2 on January 15th 2021. On that event, liquefaction phenomenon has been found on several places, triggering post liquefaction settlements in several buildings. An earthquake hazard assessment for the city is urgently needed. Unfortunately, the information related to Mamuju's earthquake hazard is still inadequate. Therefore, this study aims to assess liquefaction potential for the city of Mamuju. A series of geotechnical investigations were undertaken consisting of a number of boreholes and N-SPT measurements. For liquefaction assessment, the following methods for estimating cyclic resistance ratio ($CRR_{M=7.5}$) were used: NCEER (1996), Vancouver Task Force (2007), Chinese Code, Japanese Highway Bridge Code, Shibata (1981), Boulanger & Idriss (2014), Cetin et al. (2004), Seed et al. (1983), Tokimatsu & Yoshimi (1983), and Kokusho et al. (1983). For the estimation of cyclic resistance ratio (CSR), the Simplified method by Seed (1974) was employed. The results show that the coastal areas in the city have high level of susceptibility to liquefaction. The liquefaction thickness of the ground is estimated to be around 8 m deep for a 0.367g seismic acceleration (200 years return period earthquake), and 10 – 16 m for 0.414g seismic acceleration (deterministic Mw 7.0 of Fault Mamuju). Ground settlement induced by liquefaction was computed based on empirical chart by Ishihara & Yoshimi (1992). It was estimated that the ground settlement could be between 18 – 50 cm, and 31 – 71 cm for each assumed seismic acceleration. The validity of the methods used in this study were examined through the comparation of predictive liquefaction thickness and ground settlement based on the empirical methods with the measured ones in the field.

KEYWORDS Sulawesi Earthquake; liquefaction; Mamuju; N-SPT based methods

1 INTRODUCTION

1.1 6.2 Mw Mamuju Earthquake 2021

Sulawesi is one of the large islands in Indonesia Archipelago; the island is also prone to major earthquakes. This is due to the island being situated at the conjuncture of several active tectonic plates, including Australian, Pacific, Eurasian and Philippine Sea plates. A major earthquake, with a moment magnitude of Mw 6.2, occurred on January 15th, 2021, in West Sulawesi. The earthquake inflicted devastating impacts on many buildings, causing buildings to collapse as well as slope failures. Most of the damages occurred in Mamuju City, the capital city of West Sulawesi Province (Fig. 1). Despite the significant damage caused by the earthquake, the earthquake can be categorized as a low magnitude earthquake. One of the main earthquake-induced phenomena in the 2021 Mamuju Earthquake is liquefaction induced ground settlements. This phenomenon was seen in many places in Mamuju City, including banks, offices, hotels, automotive showroom buildings, commercial stores, and hospitals. This is to be expected as the ground conditions of the city are mainly deep alluvium of loose sands. In addition, the city is adjacent to several active faults. This study aims to further assess the liquefaction potential of Mamuju City by using SPT-Based liquefaction assessment methods.

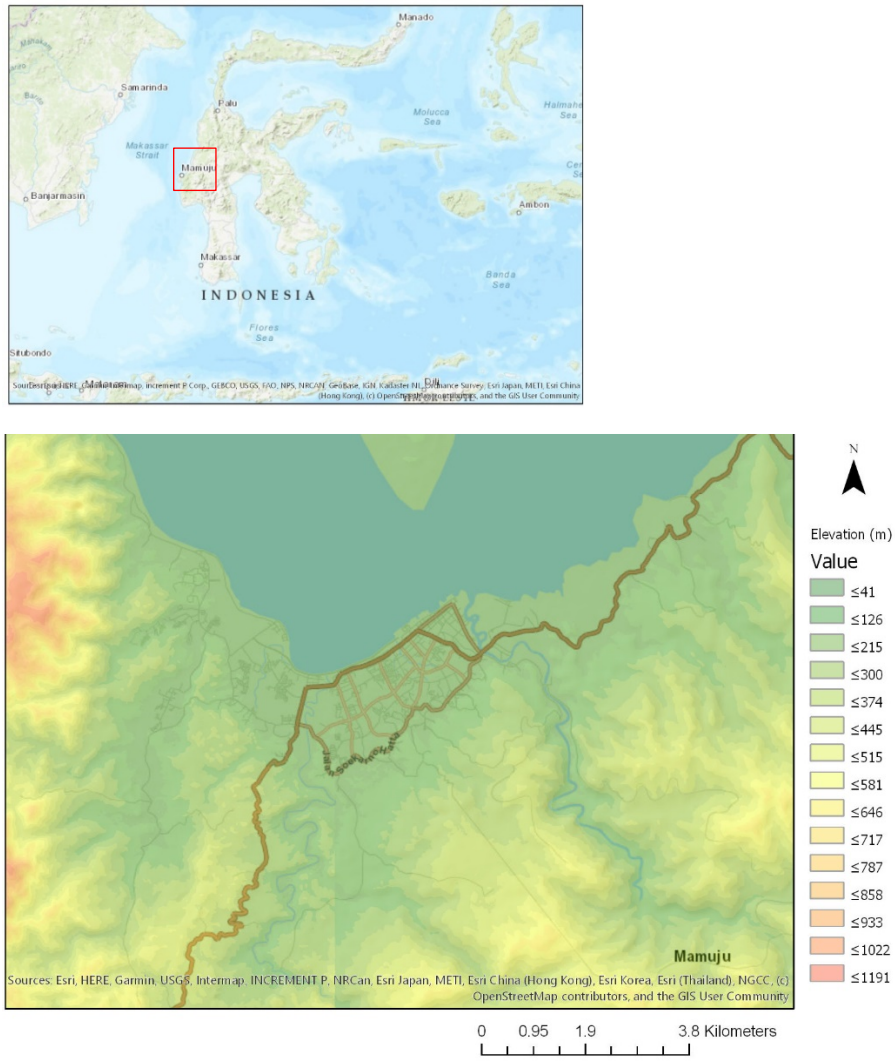

Figure 1. Location of study area, Mamuju City, West Sulawesi Province.

1.2 Geological Condition

The city of Mamuju is located at alluvial ground, surrounded by volcanic rock complex of Adang (Tma) and sedimentary rock of Mamuju (Tmm) (Fig. 2). The bedrock in this region is andesitic-basaltic, originated from active continental margin South West Microcontinent. The Adang volcanic complex (Tma) is dominantly composed by tuff, lapilli-tuff, agglomerate, volcanic breccia, volcanic-sedimentary products (Godang et al., 2016), while sedimentary rock of Mamuju (Tmm) consists of claystone and sandstone. Regarding alluvial ground where most of the city is located, thick sand layers in the ground originated from the deposition of transported sediments from several rivers across the city, including River of Karama, River of Mamuju, River of Simboro (Qa).

1.3 Seismotectonic Condition

The city of Mamuju is adjacent to several seismically active faults, including Makassar strait thrust (MST) fault, Mamuju thrust (MT) fault, and Somba thrust fault (Fig. 3). The Mamuju thrust is considered to be very near the city (11.70 km) with a slip rate of 2 mm/year, and maximum magnitude Mw. 7. Being close to the active faults, the city has experienced many large earthquakes, such as Mw 7.0 on 23 February 1969 and Mw 7.0 on 8 January 1984. The epicenter of Mw 6.2 earthquake on 15 January 2021 is also located relatively near the epicenter of the previous two large earthquakes.

Figure. 2. Geology condition of Mamuju. (Ratman & Atmawinata, 1993)

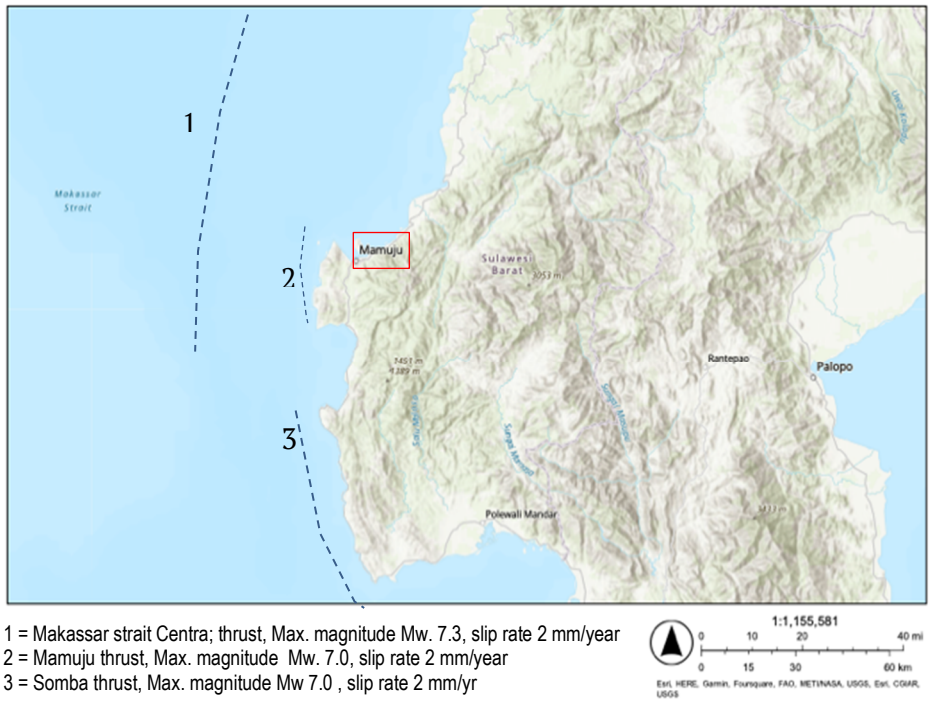

Figure. 3. Active faults are adjacent to Mamuju (Pusat Studi Gempa Nasional, 2017)

2 METHODS OF N-SPT BASED LIQUEFACTION ASSESSMENTS

Liquefaction susceptibility of a studied area can be assessed quantitively by using two approaches. First, evaluation of stress induced by earthquake and stress causing liquefaction can be conducted through cyclic laboratory tests. Second, empirical methods are undertaken in which in-situ soil strength measurement is compared to the field performance of a site in previous earthquake. Since the empirical methods of in-situ measurement are more economical with less potential disturbance than the laboratory test-based method, the empirical methods are preferred and more widely implemented. The empirical method that is generally practiced is based on standard penetrations tests (SPTs). In this method, liquefaction resistance, represented by cyclic resistance ratio (CRR), is estimated through correlations of CRR with N-SPT measurements derived from large data-base of liquefaction catalogs.

The most comprehensive liquefaction catalogs was developed by Seed and Idriss (1971), Seed et al. (1977), Seed et al. (1981), Seed and Idriss (1981, 1982), and Seed et al. (1983, 1984), and also by Tokimatsu and Yoshimi (1983). The empirical chart of standardized SPT blow-count $(N_1)_{60}$ and cyclic stress ratio (CSR) was introduced by Seed et al. (1985). In 1996, the National Center for Earthquake Engineering Research (NCEER) reviewed the empirical methods of liquefaction resistance (CRR) estimation and introduced a flowchart for evaluating the liquefaction potential (Fig. 4). Besides the NCEER method, later development of N-SPT based liquefaction assessment method contributed to at least another 10 methods, including Japanese Highway Bridge Code, Vancouver Taskforce (2007), and Boulanger & Idriss method (2014). The method of quantifying liquefaction potential with N-SPT based CRR can be seen in Table 1.

For estimating cyclic stress ratio (CSR), Simplified Seed (1974) was used (Eq. 1). Since the CSR and CRR7.5 are provided for earthquake magnitude of 7.5, a magnitude scaling factor was used to adjust its value for the target earthquake magnitude (Eq. 2 and 3). In this study, Idriss, NCEER (1997) a magnitude scaling factor (MSF) formula was used (Eq. 4 and 5). Depth reduction factor and relative density were determined by using Idriss (1999) and Idriss & Boulanger (2003) formula.

$$CSR = 0.65 \frac{a_{max}}{g} \frac{\sigma_{v0}}{\sigma'_{v0}} r_d \quad (1)$$

$$100.CRR_{M=7.5} = \frac{95}{34-(N_1)_{60}} + \frac{(N_1)_{60}}{1.3} - \frac{1}{2} \quad (2)$$

$$CRR = CRR_{M=7.5} * MSF \quad (3)$$

For Mw < 7.0 $$MSF = 10^3 * {M_w}^{-3.46} \quad (4)$$

For Mw ≥ 7.0 $$MSF = 10^{2.24} * {M_w}^{-2.56} \quad (5)$$

$$r_d = 1.0 + 1.6 * 10^{-6}(z^4 - 42z^3 + 105z^2 - 4200z) \quad (6)$$

$$FS = \frac{CRR}{CSF} K_\sigma K_\alpha \quad (7)$$

Where:

g = acceleration due to gravity (9.81 m/s^2)

a = seismic acceleration (g)

σ_{v0} = total vertical burden stress (kPa)

σ'_{v0} = effective vertical burden stress (kPa)

$CRR_{M=7.5}$ = cyclic resistance ratio for a Mw = 7.5 earthquake

$(N_1)_{60}$ = the corrected clean sand equivalent SPT value

MSF = Magnitude scaling factor

CRR = cyclic resistance ratio of the soil for an earthquake magnitude corresponding to MSF.

R_d = stress reduction factor

z = the depth below the ground surface in meters

K_σ = overburden stress correction factor

K_α = ground slope correction

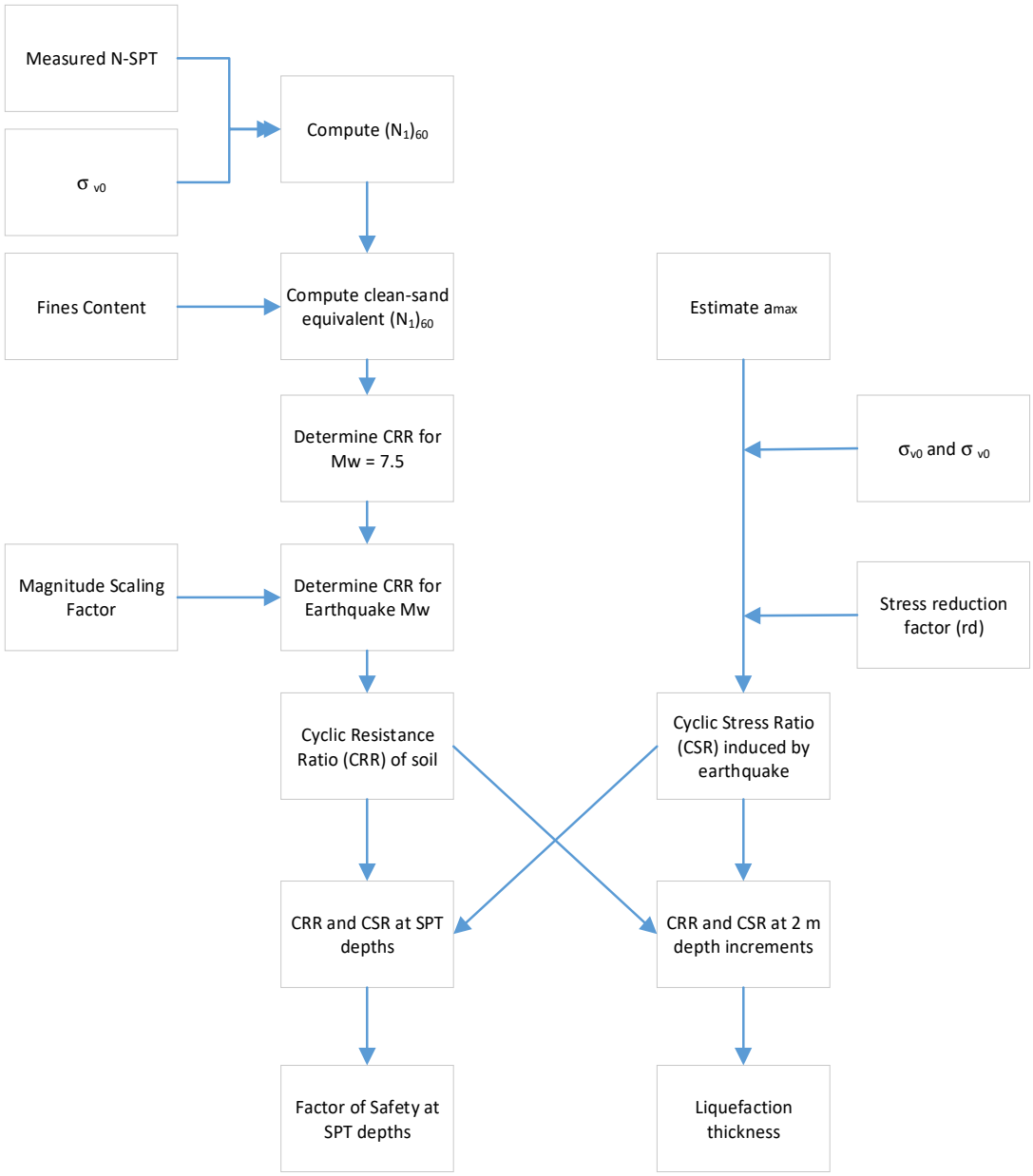

Figure. 4. Flowchart of estimating liquefaction potential based on N-SPT (NCEER, 1996).

Table 1. N-SPT based Liquefaction Assessment Methods

No	Method	Year	$CRR_{M=7.5}$
1	NCEER Workshop	1997	$100.CRR_{M=7.5} = \frac{95}{34-(N_1)_{60}} + \frac{(N_1)_{60}}{1.3} - \frac{1}{2}$
2	Vancouver Task Force	2007	Similar to NCEER Workshop, except $K_\sigma = \left(\frac{\sigma'_v}{P_a}\right)^{f-1}$ (in eq. 7) where $f = 1 - 0.005Dr.$ for 40% < Dr < 80%. $CRR = CRR_1 K_m K_\sigma K_\alpha$
3	Chinese Code	-	Similar to Seed and Idriss (1983), except $N_{req} = N_0\beta[ln(0.6d_s + 1.5) - 0.1d_w]\sqrt{\frac{3}{\rho_c}}$ for $d_c \le 20$ m $\beta = 0.25M - 0.89$
4	Japanese Highway Bridge Code	-	0.05mm < D_{50} < 0.6 mm $CRR_1 = 0.0882\sqrt{\frac{N_{1_{60}}}{\sigma'_v+0.7} + 0.255log\frac{0.35}{D_{50}} + R_3}$ 0.66mm < D_{50} < 2mm $CRR_1 = 0.0882\sqrt{\frac{N_{1_{60}}}{\sigma'_v+0.7} - 0.05}$ Fc < 40%, $R_3 = 0$ Fc ≥ 40%, $R_3 = 0.004F_c - 0.16$
5	Shibata	1981	$\frac{\tau_{max}}{\sigma'_v} = a\{N_1{}^{0.5} + (bN_1)^n - 14.8f(D_{50})\}$
6	Boulanger & Idriss	2014	$CRR_{\sigma=1,\alpha=0} = e^{\left\{\frac{(N_1)_{60}}{14.1}\right\} + \left(\frac{(N_1)_{60}}{126}\right)^2 - \left(\frac{(N_1)_{60}}{23.6}\right)^3 + \left(\frac{(N_1)_{60}}{25.4}\right)^4 - 2.8}$
7	Cetin et al.	2004	$CRR = \exp\left[\frac{(N_1)_{60}(1 + 0.004FC) + 0.05FC - 29.53\ln(M_w) - 3.70\ln\left(\frac{\sigma'_v}{P_a}\right) + 16.85 + 2.70\phi^{-1}(P_L)}{13.32}\right]$
8	Seed et al.	1983	$CRR = CRR_{\sigma=1.0,\alpha=0} K_\sigma K_\alpha$
9	Tokimatsu & Yoshimi	1983	$\frac{\tau_l}{\sigma'_0} = aC_r\left[\frac{16\sqrt{N_1+\Delta N_f}}{100} + \left(\frac{16\sqrt{N_1+\Delta N_f}}{C_s}\right)^n\right]$ Where a = 0.45, C_r = 0.57, n = 14, ΔN_f = 0 for clean sand, and ΔN_f = 5 for silty sand.
10	Kokusho et al.	1983	$\frac{\tau_{max}}{\sigma'_v} = a\{N_1{}^{0.5} + (bN_1)^n - 14.8f(D_{50})\}$ $f(D_{50}) = 0.225log_{10}(D_{50}/0.35)$ 0.04 ≤ D50 ≤ 0.6 mm $f(D_{50}) = 0.05$ 0.6 ≤ D50 ≤ 1.5 mm

2.1 Boreholes Data

Geotechnical drillings were undertaken to reveal the subsurface conditions in the city, particularly in the coastal area of the city. From a total of 10 boreholes, only 5 boreholes were studied for specific coastal area in Mamuju (Fig. 5). Fig. 6 shows the N-SPT results from the boreholes. The first 8 m thick is very loose silty sands, underlain by 10 m thick of loose silty sand, underlain by 26 m thick of medium dense sands, underlain by 10 m thick of dense – very dense sands. Laboratory tests were also performed on several soil samples obtained from the drillings (Table 2). The subsurface is dominated by fine sands with minor non-plastic silt. Groundwater level is located at -2.00 m from the ground surface.

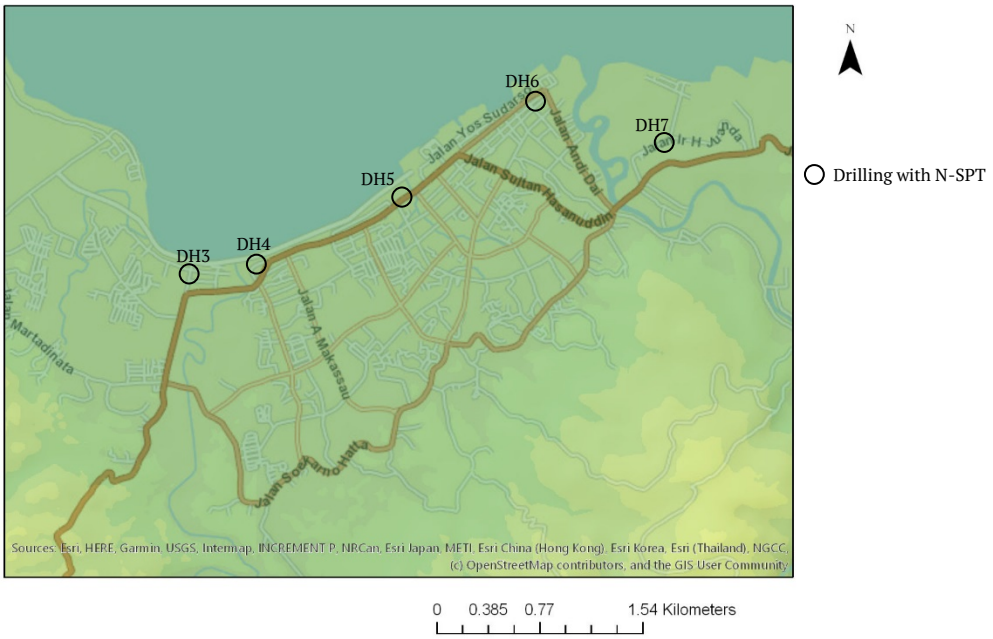

Figure 5. The location of geotechnical drillings.

2.2 Seismic acceleration for liquefaction assessment

Seismic accelerations used in the study, is in accordance with probabilistic and deterministic seismic accelerations which were investigated in previous studies (Rantesalu, 2021, Pabendan 2021). The peak ground acceleration (PGA) was deterministically estimated to be 0.459g, considering the Fault of Mamuju location of 11 km from the city, and maximum earthquake of Mw. 7.0. Given by the amplification factor of 0.9 for Site Class E (SNI-1726 2019), the peak surface acceleration (PSA) can be calculated as 0.414g (Table 3). Besides deterministic PGA, the probabilistic PGAs were also estimated for return periods of 200, 500, 2500, 5000, and 10000 years. For 200 years return period, the PGA and PSA were estimated about 0.35g and 0.3675g, based on the amplification factor of 1.05.

Table 2. Laboratory tests of boreholes soil samples.

Soil Physics and Mechanics Parameter	Boreholes				
	DH 3	DH 4	DH 5	DH 6	DH 7
Unit weight (kN/m^3)	15.50	14.60	18.50	15.30	18.10
Water content (%)	12.76	15.55	24.94	16.87	16.36
Coarse sand (%)	0	0	0	6.22	5.05
Medium sand (%)	12.12	21.88	29.14	12.12	19.08
Fine sand (%)	66.7	65.19	57.79	64.33	72.41
Non-Plastic silt (%)	21.18	12.93	13.07	17.33	2.66
USCS Classification	SM	SM	SM	SM	SP
Coefficient of uniformity	5.27	7.74	8.84	7.98	3.72
Average SPT	9.43	8.77	7.58	8.73	14.29
D_{50} (mm)	0.13	0.28	0.32	0.30	0.28
Internal friction angle, ϕ (º)	23.7	29.7	29.1	30.16	28.20

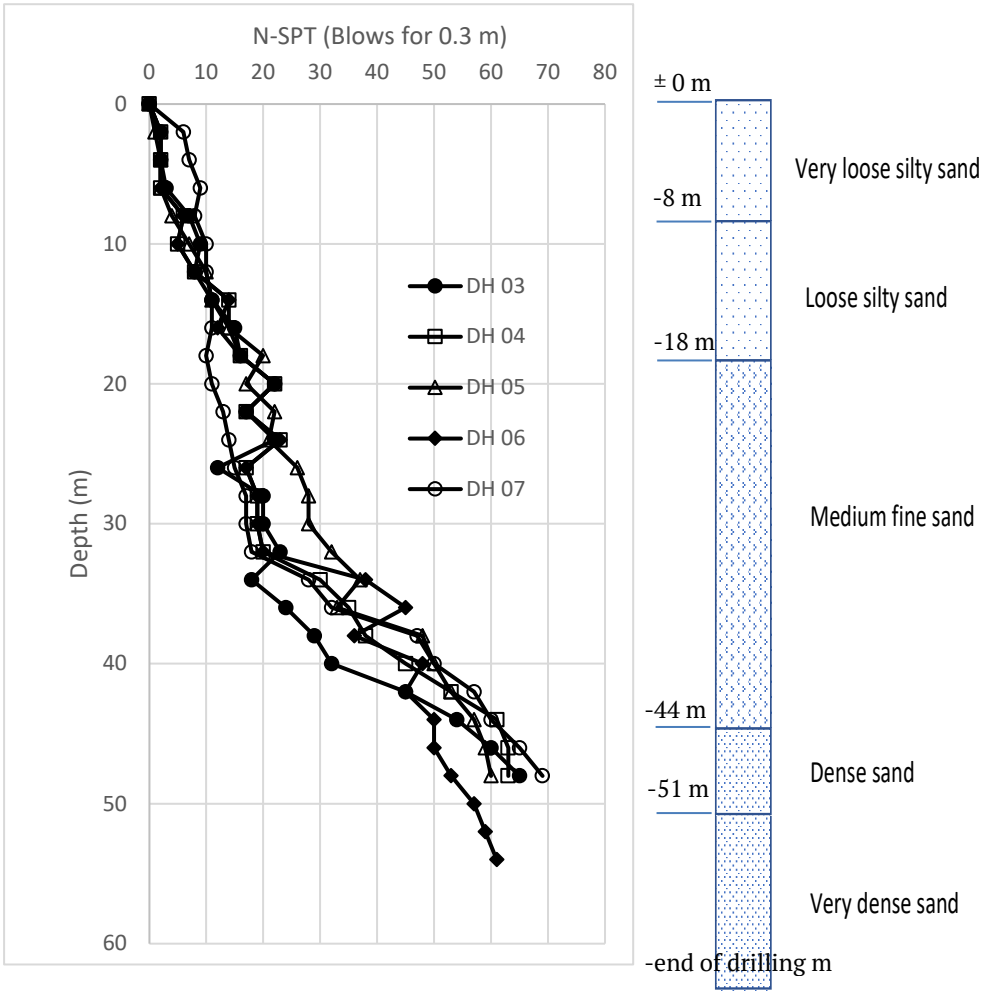

Figure 6. N-SPT blow-counts in geotechnical drillings.

Table 3. Deterministic and probabilistic based seismic acceleration at bedrock (PGA) and ground surface (PSA).

Return Period (years)	Computed PGA (g)	Peak ground acceleration (PGA) (g) based on SNI 1726-2019	Amplification factor (Fa)	Peak surface acceleration (PSA) (g)
200	0.35	0.2 – 0.25	1.05	0.3675
500	0.48	0.4 – 0.5	0.9	0.414
2,500	0.68	0.9 – 1.0	0.9	0.612
5,000	0.78	1.0 – 1.2	0.9	0.702
10,000	0.89	1.2 – 1.5	0.9	0.801
Deterministic	0.46	0.8 – 0.9	0.9	0.413

3 RESULTS

The empirical models of liquefaction potential assessment methods were utilized to predict the occurrence of liquefaction and liquefaction thickness at each SPT-borehole location. Before that, the N-SPT blow-counts were corrected to a standardized value of $(N_1)_{60}$ by using a recommended factor given by Robertson and Fear (1996) as shown in Eq. 8. The CRR, CSR, safety factor, and probability of liquefaction were processed by using the software Novoliq (Novotech, 2022).

$$(N_1)_{60} = N_{SPT}.C_N.C_E.C_B.C_S.C_R \quad (8)$$

Where:

N_{SPT} = SPT's blow count per foot.

C_N = correction factor due to normalized blow counts to overburden pressure, $C_N = \sqrt{\frac{P_a}{\sigma'_v}} \leq 2.0$

C_E = correction factor due to the energy efficiency, $C_E = ER/60$

C_B = correction factor due to the diameter of borehole

C_S = correction factor due to sample liner

C_R = correction factor due to rod length

3.1 Corrected N-SPT Blow-counts

The correction for overburden stress (C_N) is based on Seed (1976), while the correction for energy efficiency (C_E) delivered by SPT hammer is used based hammer type and hammer release and energy ratio. Seed et al. (1985) has given specific values when the measurement of energy ratio is not available. For other corrections factors: borehole diameter correction (C_B), sample liner (C_R) and loss of energy due through reflection of short length drill rod, corrections proposed by Robertson and Fear (1996) are used. The results of corrected blow-counts can be seen in Figs. 7a, 8a, 9a, 10a, and 11a.

3.2 Cyclic resistance ratio and cyclic stress ratio

In the liquefaction potential assessment, cyclic resistance ratio (CRR) was quantified based on the computed clean-sand equivalent $(N_1)_{60}$. This is done by using *several* $CRR_{M=7.5}$ - $(N_1)_{60}$ relations as seen in Table 1. The results can be seen in Figs. 7b, 8b, 9b, 10b, and 11b. The computed CRRs based on the NCEER method and the Vancouver taskforce are very similar, showing lower bound results, while the computed CRRs based on the Japanese Highway bridge method is the upper bound. The rest of the computed CRRs are in between the two bounds. This similarity of NCEER and the Vancouver taskforce are due to the same correlation of $CRR_{M=7.5}$ - $(N_1)_{60}$ being used. The minor difference between the two is from the modification in Vancouver taskforce method on the overburden stress correction factor (K_σ) to include the influence of sand relative density. These methods resulted in the minimum CRRs since the $CRR_{M=7.5}$ - $(N_1)_{60}$ correlation equations do not consider the effects of the mean of grain size distribution of sand on the cyclic shear resistance ratio (CRR). The effect of grain size of sand and fine content is accounted for in the Japanese Highway bridge method. The smaller the average grain size, the larger the CRR value is. In contrast, the larger the average grain size, the lower the CRR value is.

It must be noted that the method introduced by Cetin et al. (2004) is excluded from the list of results as it shows much higher results. This is because, as stated by Idriss and Boulanger (2010), the Cetin et al. (2004) method should be used with careful consideration of overburden correction factors (K_σ, r_d, and C_N). Otherwise, the calculated value of CRR/CSR ratio would unrealistically large.

From the results, it can be drawn that the CRR calculated based on the NCEER method gives lower bound result, while the CRR calculated based on the Japanese Highway Bridge Code gives the upper bound for fine sand layer. The Shibata (1981) and the Kokusho et al. (1983) methods generated CRRs of median values. However, for medium sand, the Seed et al. (1983) based CRR becomes the upper bound (26 m depth for DH5, Fig. 9), while the NCEER based CRR is consistently at the lower bound. In contrast, for dense sand, the Japanese Highway Bridge Code generated a lower bound CRR, while the Vancouver Task Force generated an upper bound CRR (Figs. 7 – 11). In this study, all the CRR methods were averaged as average $CRR_{M=7.5}$ (dark grey line with circle mark) and multiplied by magnitude scaling factor for the maximum Mw 7.0.

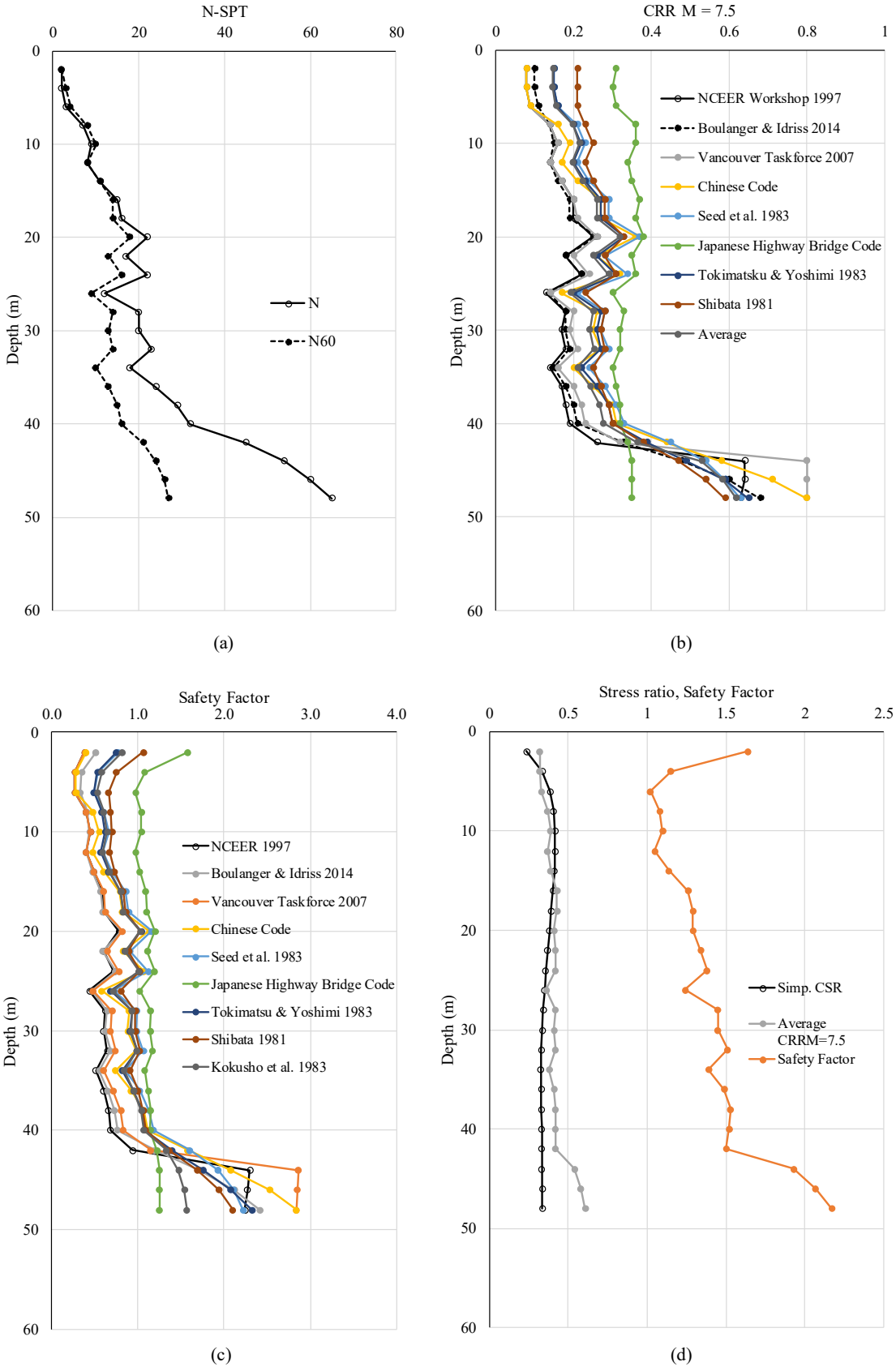

Figure. 7. (a) N-SPT and $(N_1)_{60}$, (b) Computed $CRR_{M=7.5}$, (c) SF, and (d) CRR/CSR for the site of DH 3.

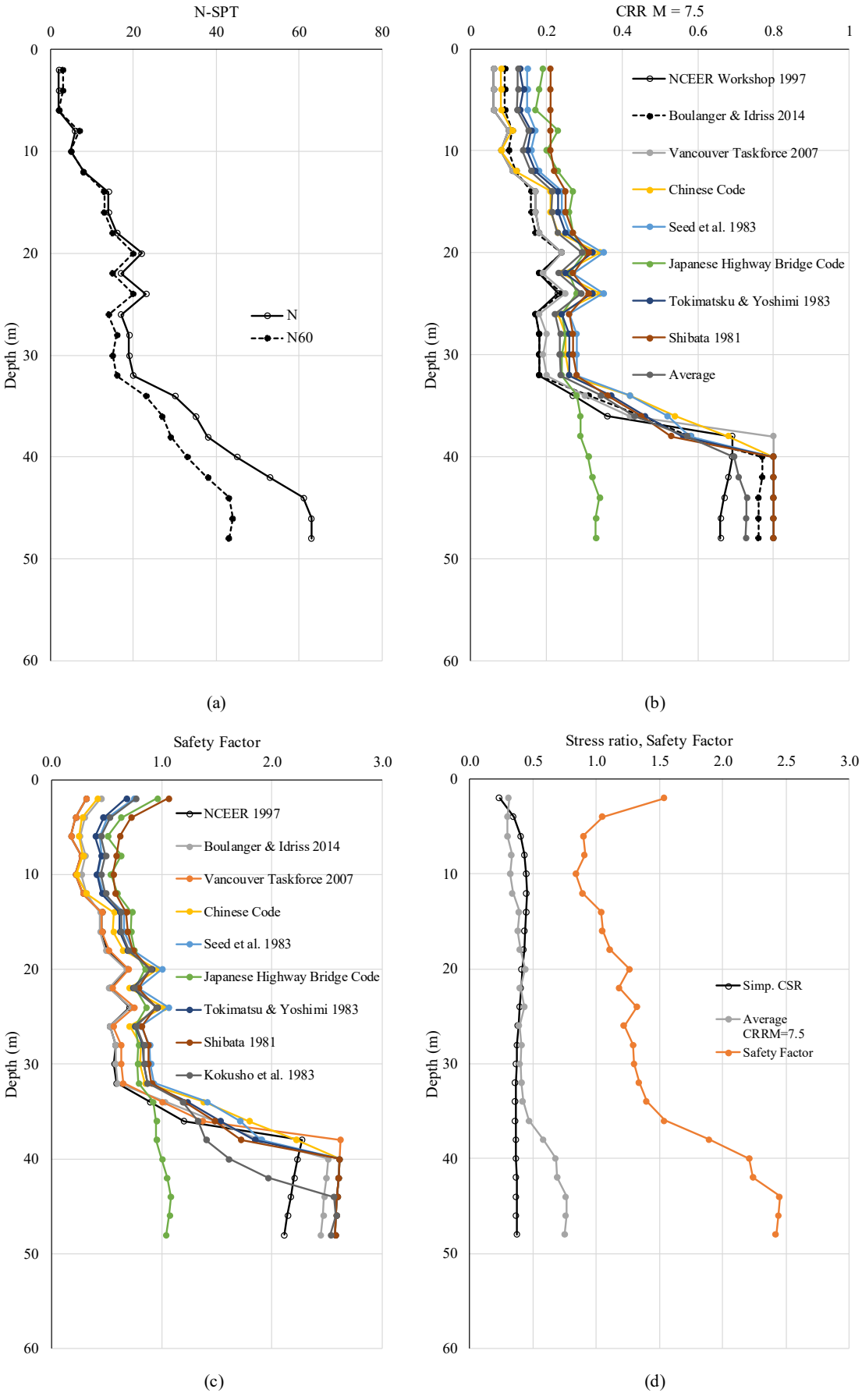

Figure. 8. (a) N-SPT and $(N_1)_{60}$, (b)Computed $CRR_{M=7.5}$, (c) SF, and (d) CRR/CSR for the site of DH 4.

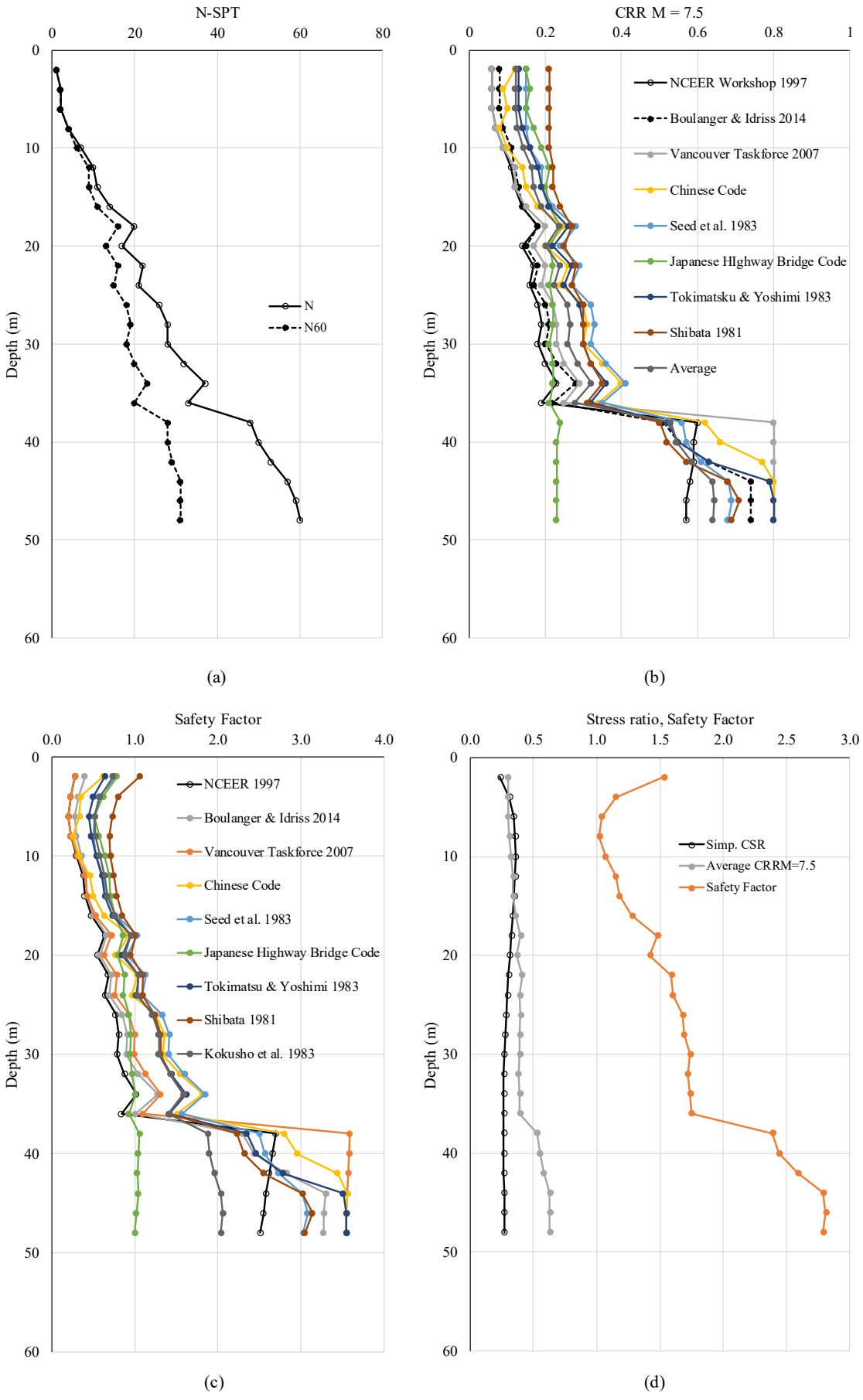

Figure. 9. (a) N-SPT and $(N_1)_{60}$, (b)Computed $CRR_{M=7.5}$, (c) SF, and (d) CRR/CSR for the site of DH 5.

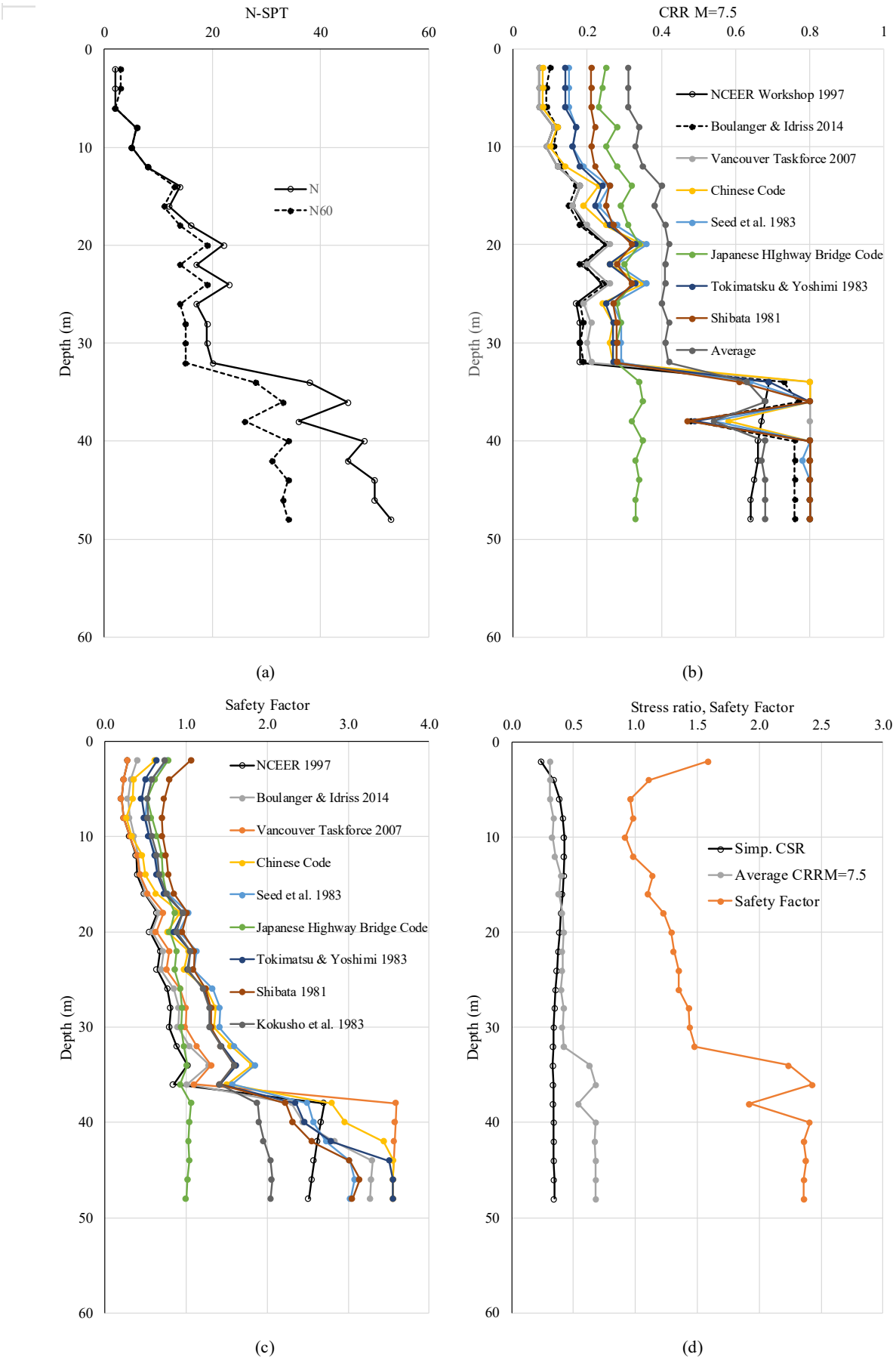

Figure. 10. (a) N-SPT and $(N_1)_{60}$, (b)Computed $CRR_{M=7.5}$, (c) SF, and (d) CRR/CSR for the site of DH 6.

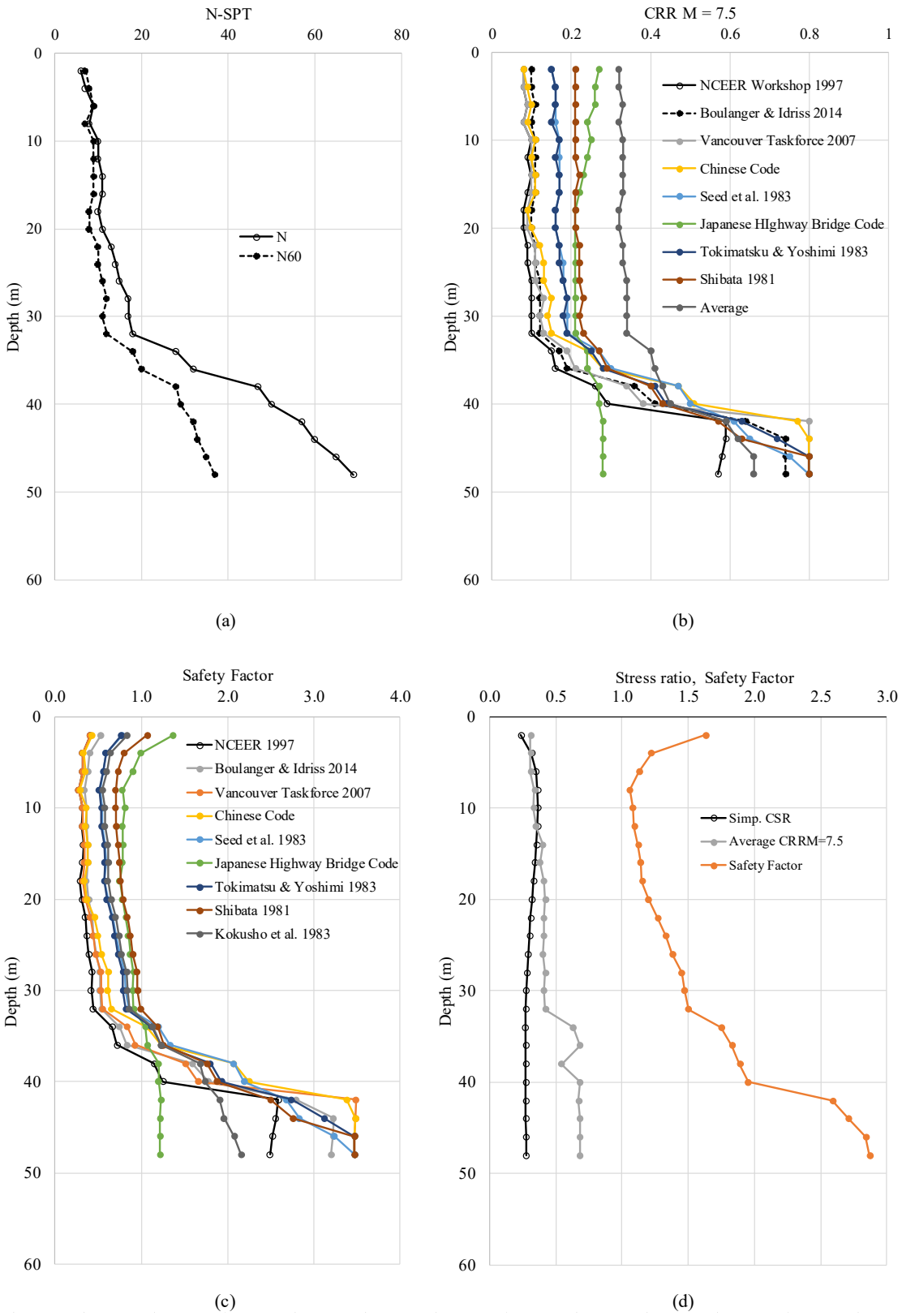

Figure. 11. (a) N-SPT and $(N_1)_{60}$, (b)Computed $CRR_{M=7.5}$, (c) SF, and (d) CRR/CSR for the site of DH 7.

Cyclic stress ratio (CSR) induced by earthquake was computed by using the Simplified CSR. The maximum seismic acceleration (a_{max}) was derived from deterministic seismic acceleration and 200 years return period probabilistic seismic acceleration at ground surface considering amplification factor. The computed CRR was divided by the computed CSR in order to obtain a factor of safety (FS), defining liquefaction potential. The FS obtained from each methods are shown in Fig. 7c, 8c, 9c, 10c, and 11c, while the average CRR, simplified CSR and average factor of safety are shown in Fig. 7d, 8d, 9d, 10d and 11d. From figure 7d-11d, it can be seen that for DH3 and DH 4, the computed CSR > CRR starting from 18 m depth, while in the DH 5, DH 6, and DH 7 the computed CSR > CRR starting from 10 m, 16 m, and 16 depth, respectively.

For the earthquake conditions in City of Mamuju, PSA of 0.367 (probabilistic 200 years return period seismic acceleration), the liquefaction thickness is similar for all boreholes, calculated to be 8 m thick (Table 4). If PSA equal to 0.414g from deterministic seismic acceleration is used, the liquefaction thickness becomes 10 m to 16 m. Borehole DH 4 generates the thickest liquefaction thickness among the boreholes. The probability of liquefaction was determined based on Youd & Noble (2002), as shown in Eq. 9. The results show that the probability of liquefaction is very high (90 - 97%) for the liquefaction thickness of each borehole (Table 4). Liquefaction induced ground settlement was computed based on Ishihara & Yoshimi (1992)'s chart, in which volumetric re-consolidation strain ranges from 4.5% for loose sand to 1% for very dense sand. Compared to other boreholes, DH 03 is the borehole which would generate the largest liquefaction induced ground settlement, while DH07 would generate lowest ground settlement.

$$Logit\ (PL) = ln(PL/(1-PL)) = 7.633 + 2.256M_w - 0.258N_{1(60)} + 3.095ln(CRR) \qquad (9)$$

where

PL = the probability that liquefaction occurred

Table 4. Liquefaction thickness and probability of liquefaction.

Probabilistic	M = 7.0. PSA = 0.367g		
DH	Liquefaction Thickness (m)	Probability of Liquefaction	Post liquefaction Settlement (cm)
03	8	90.5% - 97.2%	50
04	8	89.4% - 96.0%	49
05	8	87.5% - 95.1%	16
06	8	90% - 95%	38
07	8	91.1% - 93.8%	18
Deterministic	M = 7.0. PSA = 0.414g		
03	14	81.8% - 97.2%	71
04	16	70.8% - 95.9%	64
05	10	87.4% - 96.5%	42
06	10	87.5% - 95.1%	54
07	10	91.1% - 93.8%	51
Validation	M = 6.2, PSA = 0.26g		
Building	6	100% (already happened)	31 (calculated by the software) 30 – 40 cm (measured)

3.3 Validation of liquefaction induced ground settlement in 2021 Mamuju Earthquake Mw. 6.2

To validate the liquefaction assessment explained in the previous section, similar N-SPT based liquefaction assessment methods were also used on a building located in the near petrol station in Mamuju. The building has suffered post liquefaction settlement during the earthquake 15 January 2021. The calculated and measured liquefaction-induced ground settlement are compared. The drilling with N-SPT and site measurement of the building were undertaken. The elevation measured is shown in Fig. 12. The measured post liquefaction ground settlement of the building is ranging from 30 to 40 cm where the minimum settlement 30 cm located at the corner column of the service room, and the maximum 40 cm settlement located at the column of the office in the building. The PGA from BMKG time histories was 0.14g. Given the amplification factor, the PSA at the time of earthquake is estimated to be 0.26g. By using the aforementioned N-SPT liquefaction assessment methods, the liquefaction thickness was estimated to be 6 meters deep (Table 4), and the calculated liquefaction-induced ground surface settlement is about 31 cm. The result of the assessment and the measurement in the field are in well agreement. The results suggested that the methods used in this study can be further implemented for predicting liquefaction in future earthquakes around the city.

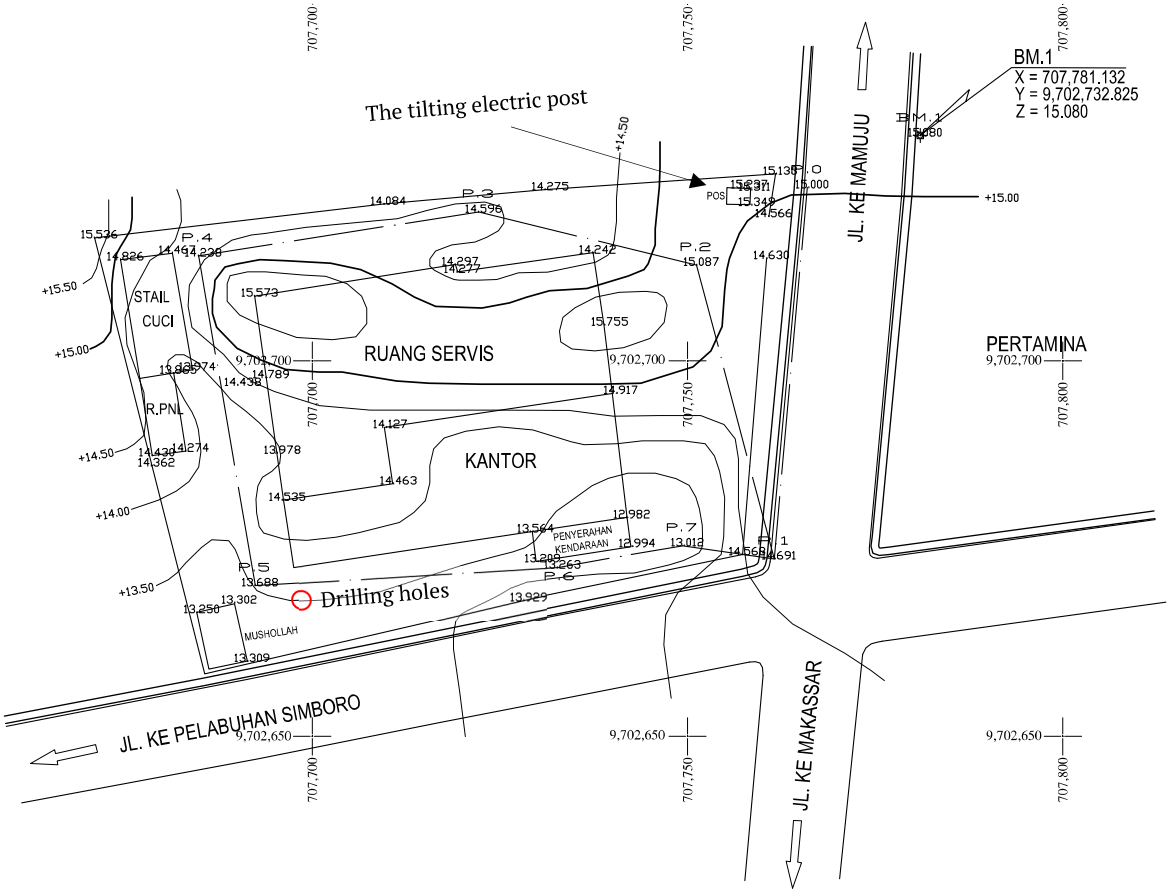

(a)

(b)

Figure. 12. (a) site measurement of ground settlement around the building indicated around 30 cm settlement, (b) tilting electric post due to post liquefaction settlement, near the building.

4 CONCLUSIONS

Liquefaction potential assessment based on N-SPT measurement for the city of Mamuju is conducted through a number $CRR_{M=7.5}$ empirical correlations catalogs with simplified CSR and magnitude scaling factor. Several findings can be drawn as follows:

- Coastal area of the city is dominantly loose fine sand with minor non-plastic silt, underlain by medium sand. The ground is categorized as Site Class E.
- Computed $CRR_{M=7.5}$ based on the empirical methods by Japanese Highway Bridge gives the upper bound results, while NCEER method gives the lower bound results for loose sand.
- Based on the average CRR with magnitude scaling factor and the CSR with deterministic and probabilistic maximum seismic acceleration, the liquefaction thickness obtained is 8 m for 0.367g seismic acceleration, and 10 – 16 m for 0.414g seismic acceleration.
- The calculated liquefaction-induced ground settlement ranges from 18 to 50 cm for 0.367g seismic acceleration, and 31 to 71 cm for 0.414g seismic acceleration.
- The assessment is validated with the measured liquefaction-induced ground settlement of a building due to the 2021 Mamuju Earthquake Mw. 6.2. The results show that the liquefaction assessment based on N-SPT methods is in well agreement with the observed liquefaction that occurred in the field.

DISCLAIMER

The authors declare no conflict of interest.

AVAILABILITY OF DATA AND MATERIALS

All data are available from the author.

REFERENCES

Boulanger, R.W. and Idriss, I.M., 2014. SPT-Based Liquefaction Triggering Procedures. Report for Center for Geotechnical Modelling. Department of Civil and Environmental Engineering, University of California, Davis, pp. 484–491.

Cetin, K.O., Seed, R.B., Der Kiureghian, A., Tokimatsu, K., Harder, L.F., Kayen, R.E., and Moss, R.E.S., 2004. Standard penetration test-based probabilistic and deterministic assessment of seismic soil liquefaction potential. *Journal of Geotechnical and Geoenvironmental Engineering*, ASCE 130(12), pp. 1314–1340. https://doi.org/10.1061/(ASCE)1090-0241(2004)130:12(1314)

Godang, S., Fadlin, F. Priadi, B., 2016. Geochemical Signatures of Potassic to Sodic Adang Volcanics, Western Sulawesi: Implications for Their Tectonic Setting and Origin. *Indonesian Journal on Geoscience*, 3(3).

Idriss, I.M., 1999. An update to the Seed-Idriss simplified procedure for evaluating liquefaction potential. *Proceedings of TRB Workshop on New Approaches to Liquefaction, Publication No. FHWA- RD-99-165, Federal Highway Administration*.

Idriss, I.M., and Boulanger, R.W., 2003. Relating K_α and K_σ to SPT blow count and to CPT tip resistance for use in evaluating liquefaction potential. *Proceedings of the 2003 Dam Safety Conference*, ASDSO, September 7–10, Minneapolis, MN.

Idriss, I.M., and Boulanger, R.W., 2004. Semi-empirical procedures for evaluating liquefaction potential during earthquakes. *Proceedings of 11th International Conference on Soil Dynamics and Earthquake Engineering, and 3rd International Conference on Earthquake Geotechnical Engineering*, D. Doolin et al., eds., Stallion Press, Vol. 1, pp. 32–56.

Idriss, I.M., and Boulanger, R.W., 2006. Semi-empirical procedures for evaluating liquefaction potential during earthquakes. *Soil Dynamics and Earthquake Engineering,* 26(2-4), pp. 115–130. https://doi.org/10.1016/j.soildyn.2004.11.023

Idriss, I.M., and Boulanger, R.W., 2008. *Soil liquefaction during earthquakes*. Monograph MNO-12, Earthquake Engineering Research Institute, Oakland, CA, 261 p.

Idriss, I.M. and Boulanger, R.W. 2010. SPT-based liquefaction triggering procedures. Report UCD/CGM-10/02, Department of Civil and Environmental Engineering, University of California, Davis, CA (2010)

Kokusho, T., Yoshida, Y. and Esashi , Y. 1983. Seismic Stability of Dense Sand Layer (Part 2) - Evaluation Method by Standard Penetration Test -.CRIEPI Report No.383026 (in Japanese).

National Center for Earthquake Engineering Research (NCEER), 1997. Proceedings of the NCEER Workshop on Evaluation of Liquefaction Resistance of Soils, T. L. Youd and I. M. Idriss, editors, Technical Report NCEER-97-022, NCEER, NY.

Novotech (2022). *Novoliq*. NovoTech Software, North Vancouver Canada.

Pabendan, O, 2021. *Study on Seismic Hazard Assessment of Mamuju using PSHA* (in Bahasa Indonesia). Doctoral Dissertation, Univeritas Hasanuddin.

Pusat Studi Gempa Nasional (PuSGeN), 2017. *Peta Sumber dan Bahaya Gempa Indonesia Tahun 2017* (in Bahasa Indonesia). Puslitbang Perumahan dan Permukiman, Kementerian PUPR.

Rantesalu, C.R., 2021. Study on Seismic Hazard Assessment of Mamuju using DSHA (in Bahasa Indonesia). Doctoral Dissertation, Univeritas Hasanuddin.

Ratman, N., Atmawinata, S., 1993. *Geological Map of Mamuju Quadrangle Sulawesi*. Geological Research and Development Centre, Bandung Indonesia.

Seed, H.B., Ascoli, R.G., Gomez-Masso, A., Chan, C.K. and Arango, I., 1981. Earthquake-induced liquefaction near lake Amatitlan, Guatemala. *Journal of the Geotechnical Engineering Division*, 107(4), pp.501-518.

Seed, H.B., and Idriss, I.M., 1971. Simplified procedure for evaluating soil liquefaction potential. *J. Soil Mechanics and Foundations Div.*, ASCE 97(SM9), pp. 1249–1273. https://doi.org/10.1061/AJGEB6.0001122

Seed, H.B., and Idriss, I.M., 1982. *Ground Motions and Soil Liquefaction During Earthquakes*, Earthquake Engineering Research Institute, Oakland, CA, 134 p.

Seed, H.B., Tokimatsu, K., Harder, L.F. Jr., and Chung, R., 1984. *The influence of SPT procedures in soil liquefaction resistance evaluations*. Earthquake Engineering Research Center, University of California, Berkeley, Report No. UCB/EERC-84/15, 50 p.

Seed, H.B., Tokimatsu, K., Harder, L.F. Jr., and Chung, R., 1985. Influence of SPT procedures in soil liquefaction resistance evaluations. *Journal of Geotechnical Engineering*, ASCE, 111(12), pp. 1425–1445. https://doi.org/10.1061/(ASCE)0733-9410(1985)111:12(1425)

Seed, R.B., Cetin, K.O., Moss, R.E.S., Kammerer, A., Wu, J., Pestana, J., Riemer, M., Sancio, R. B., Bray, J.D., Kayen, R.E., and Faris, A., 2003. Recent Advances in Soil Liquefaction Engineering: a Unified and Consistent Framework. *Proceedings of the 26th Annual ASCE Los Angeles Geotechnical Spring Seminar, Long Beach, CA*.

Seed, H.B., Tokimatsu, K., Harder, L.F. Jr., and Chung, R., 1985. Influence of SPT procedures in soil liquefaction resistance evaluations. *Journal of Geotechnical Engineering*, ASCE 111(12), pp. 1425–1444. https://doi.org/10.1061/(ASCE)0733-9410(1985)111:12(1425)

Shibata, T., 1981. Relations between N-value and liquefaction potential of sand deposits (in Japanese). *Proc. 16th Annual Convention of Japanese Society of Soil Mechanics and Foundation Engineering*, pp. 621-624.

Tokimatsu, K., and Yoshimi, Y., 1983. Empirical correlation of soil liquefaction based on SPT N-value and fines content. *Soils and Foundations*, 23(4), pp. 56-74. https://doi.org/10.3208/sandf1972.23.4_56

Youd, T.L, and Noble, S.K., 1997. Liquefaction criteria based on statistical and probabilistic analyses. *Proceedings of the NCEER workshop on evaluation of liquefaction resistance of soils*, Technical Report NCEER-97-022, pp. 201–205.